Hypothesis

We were the first to demonstrate the existence of endothelial fenestration in the distal portion of the renal afferent arterioles (AA), which is unusual among high pressure vessels. These fenestrae are co-localized with renin producing granular epithelioid cells, so this arrangement makes it likely that the relatively large renin molecules may use these fenestrae to enter into the lumen of AA. In addition, we demonstrated that filtration passes through this fenestration providing an earlier unknown fluid movement from the afferent arteriole into the area of juxtaglomerular apparatus contributing to the GFR regulating mechanisms.

We hypothesized that the formation of fenestrae in the distal portion of AA is regulated by so far ill-understood complex mechanisms. The functional consequence of the fenestration, i.e. high permeability in the AA play an important role in renal physiology/pathophysiology of fluid dynamics, microcirculation and may have a role in the development of kidney diseases.

Aims of the research proposal

1   *In vivo* measurement of permeability and evaluation of the size of fenestrae in AA endothelium

1.1 Fluorescent-labelled dextran permeability of the renal afferent arteriole (AA) in mice

We have introduced a method for measuring the permeability of the renal afferent arteriole (AA) for fluorescence-labelled dextran in mice using multiphoton fluorescence imaging. As a first step we began to measure AA permeability of dextran with molecular weights (MW) ranging from 10 to 500 kDa to determine the approximate pore diameter and select the appropriate dextran MW for functional studies.

Results: The recent size measurements of the openings of nano-channels, as well as the endothelial permeability of labelled dextran with molecular weights (MW) ranging from 10 to 500 kDa, are in accordance with our earlier data obtained with other well-established methods.

1.2 Filtration of proteins across the glomerular capillary and AA endothelium

Fibrinogen is a large protein that cannot be filtered by the glomerulus, as – depending on the composition of its two trimers – has a molecular weight of about 340 kD. However, glomerulopathies disrupt the slit membrane of the glomerulus allowing large molecules to enter the primary urine. According to our previous experience, fibrinogen can likely be filtered and is deposited in large quantities in the glomerulus of mice with focal segmental glomerulosclerosis (FSGS). Since the afferent arterioles also contribute to the production of the total amount of filtrate, it is of importance to test if the afferent arteriolar endothelium is also affected in FSGS. For this purpose, we used fibrinogen immunohistochemistry in FSGS mice and evaluated fibrinogen deposition in various parts of the kidney.

Results: In some cases fibrinogen could be seen along the proximal tubules, and large fibrinogen deposition was present in the glomeruli of mice at the advanced phase of the disease. However, fibrinogen could not be demonstrated in any of the afferent arterioles. Therefore, the integrity of the afferent arteriolar endothelium is maintained even in serious FSGS in mice.

1.3 Plasma extravasation as a measure of endothelial permeability, in vivo

In an attempt to extend our *in vitro* results to the *in vivo* situation, we introduced a method for measuring capillary permeability, also called extravasation, in mice. We used an SPF outbred mouse strain originally developed at the Naval Medical Research Institute (Crl: NMRI BR). Male mice weighing 27-35 g were purchased from Toxicoop Ltd (Budapest, Hungary). Mice

had free access to standard rodent chow (Altromin standard diet, Germany) and tap water. The mice were anesthetized with isoflurane and the test items injected via the tail vein, and then Evans blue (10 mg/mL) was administered via the retroorbital sinus 30 min later. The animals were killed by decapitation, perfused with cold saline via the heart to wash out Evans blue containing blood from the organs, and various organs were dissected, such as lung, skin, muscle, spleen, kidney and brain. The Evans blue from labelled albumin was extracted for 48 hours in formamide, and the dye concentration of the supernatant was measured at 620 nM.

To evaluate the effects of low, normal and high sodium chloride intakes on the main factors regulating capillary permeability, and also on the main membrane protein components and regulatory factors of endothelial fenestrae and caveoli, separate groups of mice were fed low and normal sodium chloride diets, and a third group was given normal sodium diet and 1 % saline to drink, which represented high sodium chloride intake. Tissue samples were collected from the lung, skin, muscle, liver and kidney for histology and molecular biology analysis in all groups.


Results

For the introduction of the method we selected zymosan, which is a direct activator of the complement system, and also an agonist of toll-like receptor 2 (TLR2), and is known to considerably increase capillary permeability. The results clearly show that the Evans blue-stained albumin is suitable for measuring capillary permeability in vivo. Extravasation was increased in most organs measured especially in the muscle, skin and lung of zymosan-treated mice (**Figure 1A**). This method can be used to extend and generalize our *in vitro* observations to the whole animal.

Inhibition of angiotensin II type 1 receptors (AT1) decreased extravasation in the lung and skin but not in the kidney, muscle and intestine of mice fed a normal sodium diet (**Figure 1D**). The above effects of losartan were abolished in mice on high salt intake. These results are in agreement with our previous findings that angiotensin II increase capillary permeability and clearly show that under normal conditions stimulation AT1 receptors contribute to capillary dynamics in the lung and skin. Considering the limitations of the technique applied we cannot rule out subtle changes in permeability of renal afferent arterioles and/or muscle and intestine.

Plasma extravasation was similar in the skin, muscle, liver and kidney at all three levels of sodium chloride intakes (**Figure 1B**). Surprisingly, plasma extravasation in the lung was 3-fold higher on normal sodium chloride intake than on high or low sodium chloride intakes. Inhibition of angiotensin II type 1a receptors with losartan increased capillary permeability in the skin only in the group on low sodium chloride intake (**Figure 1C**). We started to measure the mRNA expression of the main factors regulating capillary permeability, and also the main membrane protein components of endothelial fenestrae and caveoli. As a first result, mRNA of plasmalemma vesicle associated protein-1 (PV-1) was similar in the kidney at all levels of sodium chloride intake. However, the scatter of the data was threefold higher in the high sodium chloride group compared to that in the low and high sodium chloride groups.

Figure 1. Plasma extravasation in NMRI mice on normal and low and high sodium intakes.
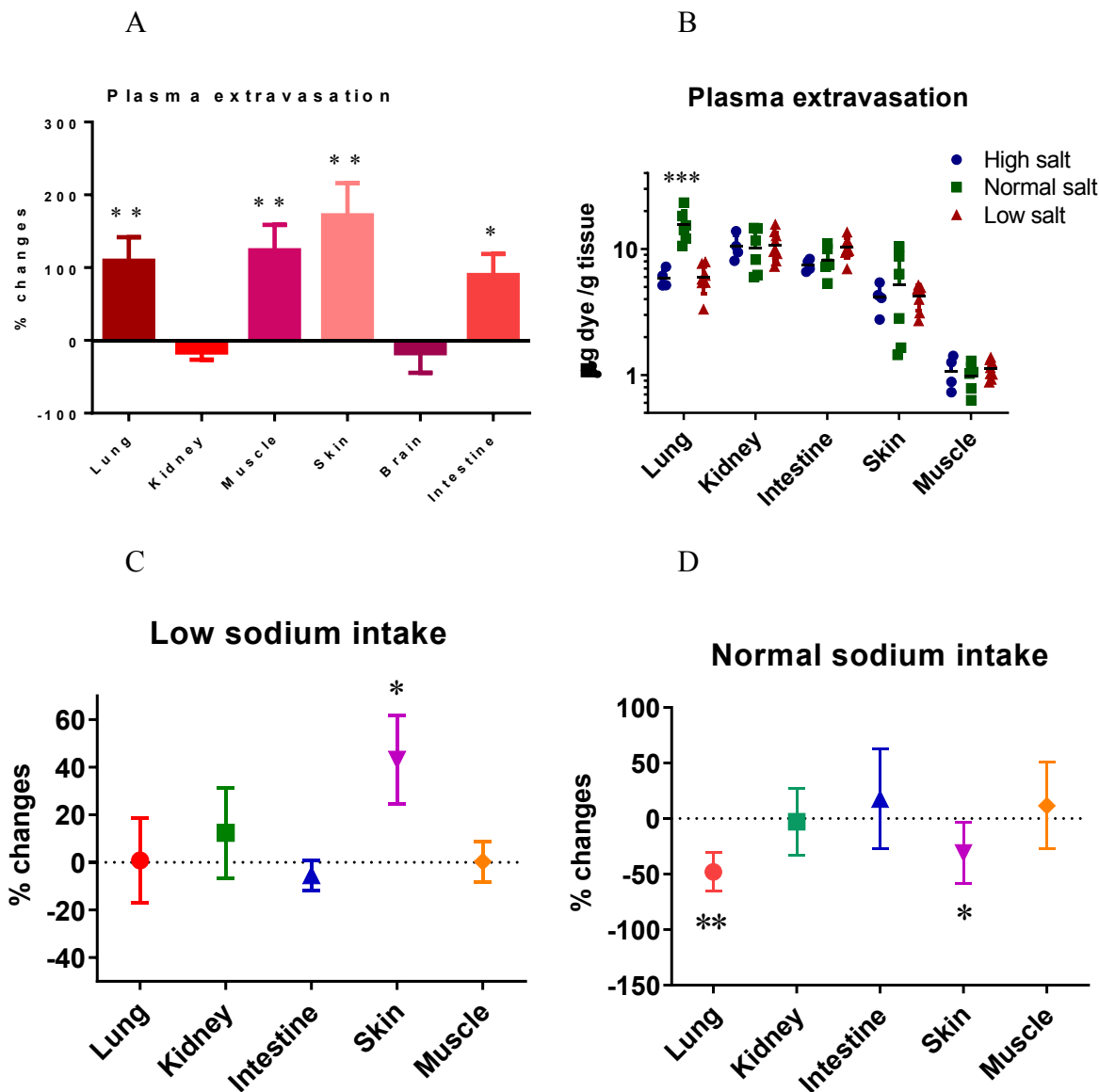
A. Effects of zymosan 30 mg/kg i.p. on plasma extravasation of various organs in mice on normal sodium; B. Effects of low, normal and high sodium intakes on plasma extravasation of various organs in mice; Effects of losartan (10 mg/kg i.p.) on plasma extravasation of various organs in mice fed low (C) and normal sodium (D) intakes. *, **, ***: $p < 0.5, 0.01, 0.001$.

Our progress during the last year was considerably delayed by the quarantine due to COVID-19 pandemic. However, during the year 2021 we plan to proceed with the planned molecular biology and histological evaluation of the organ samples collected.

2   (2-3) The role of RAS components, VEGF, TGF-β and relaxin on fenestration, permeability and composition of endothelium: intracellular signaling mechanisms modulating their effects

2.1 Effects of Ang II on endothelial permeability and PV-1 expression in CiGEnC

Plasmalemma vesicle-associated protein (PLVAP or PV-1) is specifically expressed in the endothelium, and PV-1 can be found in the diaphragm of fenestrations and caveolae. We have

previously demonstrated that treatment with angiotensin II (Ang II) for 48 hours increased endothelial permeability and PV-1 protein expression in HUVEC (Am J Physiol Cell Physiol. 2012, 302(1):C267-764).

The former experiments were repeated in conditionally immortalized human glomerular endothelial cells (CiGEnC). The cells were treated with 10-7 M Ang II and 100 ng/ml VEGF for 48 hours, *in vitro*. Endothelial permeability was measured by transwell assay using 40 kDa FITC-dextrane. Changes in PV-1 expression were evaluated using RT-PCR.

Results: Ang II markedly increased permeability and PV-1 expression in CiGENC over 1 hour and at 48 hours after treatment. Interestingly, the Ang II-induced increases in endothelial permeability and PV-1 mRNA expression were greater than those of VEGF in CiGENC, while Ang II and VEGF caused similar increases in endothelial permeability and PV-1 mRNA expression in HUVEC.

However, some unforeseen difficulties considerably delayed our progress with these experiments. A great effort was devoted to solve the following issues.

2.1.1 Technical difficulties

As the previous batch of cells had been used up, we started to work with a new batch of CiGENC kindly provided by Dr. Satchell's laboratory (UK). The new batch of cells posed great problems. The cells failed to survive the thawing procedure, just a few cells stayed alive, and the number of cells was not enough to reach confluency. In addition, the new batch of Lonza medium caused contaminations, which, after careful testing, turned out to originate from the medium. Therefore, we started to use a different endothelial growth medium purchased from another company (Cell Applications). Under the new circumstances, namely, the new batch of cells and the new medium, we had to re-optimize the FITC-Dextran permeability assay.

2.1.2 The effects of treatment time on monolayer permeability

CiGENC is a conditionally immortalized human glomerular endothelial cell line, which proliferates at 33 C and becomes growth arrested at 37 C. The cells were proliferated after seeding them on Millicell insert at 33 C for 1 and 5 days and differentiated at 37 C for 3 to 7 days. The baseline permeability of CiGENC should be optimized first in order to ensure that the cells form a fully confluent monolayer, which is a prerequisite of reliable testing of biologically active compounds on monolayer permeability.

Results: First the optimal duration of proliferation was determined. The minimum permeability of CiGEnC cells to FITC-Dextran was obtained after 5 days of proliferation shorter or longer durations resulted in larger permeability suggesting that the confluency was best if the cells started to differentiate after 5 days of proliferation. Morphology of the cells was different as well. Those monolayer cells that proliferated for 5 days were smaller in both length and diameter when compared to those proliferated for only 1 day. The minimum permeability of CiGEnC cells to FITC-Dextran was obtained when the number of cells seeded into the wells was 30.000/well; 7.500 or 15.000 cell formed less confluent cell layer, and 50.000 cells were similarly more permeable than 30.000. Permeability of CiGENC cells was lower if they were differentiated for 5 days, while 3 or 5 days were not optimal. Differentiation for 10 days increased the permeability of CiGENC cells suggesting pathological changes over long periods of differentiation. The type of coating was also optimized. If collagen type I was used permeability of CiGENC cells to FITC-Dextran was high. Permeability of CiGENC cells decreased considerably if gelatine was used for coating. The best coating proved to be fibronectin producing a permeability of about 7 % relative to cell free inserts. We also tried to optimize the duration of starvation (serum depletion) before

treatments of CiGENC cells. The cells were treated with VEGF at various concentrations and the degree and duration of starvation period was optimized. We also measured the time to reach the maximum effect of VEGF. The conclusion from this set of experiments is that starvation is important before treatments. The best results were obtained when the starvation period lasted for 3 hours, and the medium was 50 % diluted. Higher degree of dilution or longer starvation periods produced less consistent results, although the effects of VEGF on permeability were quite large in some cases. The optimal duration of VEGF treatment is 24 or 48 hours, shorter durations, especially treatment for 1 hour caused large scatter in the results.

Our researcher responsible for the cell culture experiments left us and all our efforts failed to replace her. Neither a PhD student nor a researcher skilled in cell culture experiments could be hired. In addition, the technician involved in the cell culture experiments is on maternal leave, so we had to postpone this type of studies. As an important part of the project was on hold we redesigned the studies, and asked for a one year extension of the project.

2.1.3 Effects of RAS components on endothelial permeability and PV-1 expression in HUVEC

We have started to assessed the role of renin, prorenin, angiotensin III (Ang III) and angiotensin IV (Ang IV) in fenestrae formation and modulation of permeability in HUVEC culture. HUVEC cells were treated with various doses of renin, Ang III, and Ang IV for 48 hours, *in vitro*. PV-1 protein levels were evaluated using Western blotting.

Results: All tested RAS components caused dose-dependent changes in PV-1 protein expression at 48 hours after treatment. The effect of renin and Ang III reached the level of statistical significance at the dose of 10^{-9} M (**Figure 2**), while the effect of Ang IV was statistically significant at doses from 10^{-10} M to 10^{-9} M. Since the effects of Ang IV were significant at the lower tested dose of 10-11 M, we will continue testing its effects in HUVECV to establish its lowest effective concentration. The evaluation of the effects of prorenin is in progress.

Figure 2. Time- and concentration-dependent effects of angiotensin III on PV-1 expression in HUVEC cells
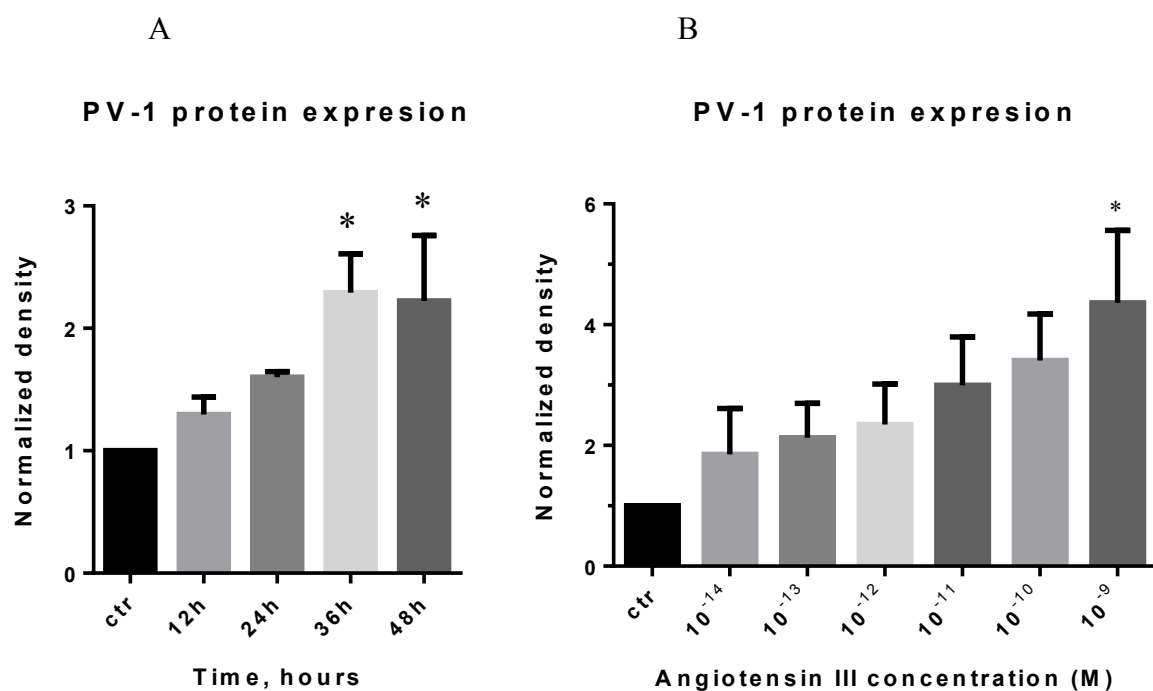
(A) Time-dependent effects of angiotensin III (10-10 M) on PV-1 expression in HUVEC cells. (B) Concentration-dependent effects of angiotensin III on PV-1 expression in HUVEC cells at 48 hours after treatment.

2.1.4 *Acute effects of Ang II on permeability and trans-phosphorylation of VEGF in HUVEC*

HUVEC cells were treated with Ang II at 10^{-7} M for 0, 1, 2, 4, 6, 8 and 10 hours and PV-1 protein levels were detected by Western blotting. Phosphorylation of VEGF at Tyr1175 was measured by Western blotting at 5, 15, 30 and 60 min after treatment with Ang II at 10-7 M.

Results: PV-1 protein levels were significantly elevated after treatment with Ang II from 1 hour to 8 hours. Treatment with Ang II trans-phosphorylated VEGFR-2 Tyr1175 at 60 min but not earlier.

2.1.5 *Effects of retinoic acid and calcitriol on VEGFR2 trafficking*

In order to better understand the complex regulation of fenestrae formation in endothelial cells we also studied the effects of retinoic acid (RA) and calcitriol (1,25-(OH)2D3) in HUVEC. The experiments demonstrated that RA and calcitriol reduced the effects of VEGF on endothelial permeability, PV-1 mRNA expression and protein levels in HUVEC (**Figures 3 and 4**). Furthermore, both vitamins blunted phosphorylation of VEGFR-2 Tyr1175 (Figure 5). We investigated the mechanism of RA and calcitriol on VEGFR-2 trafficking. HUVEC cells were grown onto confocal chambers and treated with 0.1 nM calcitriol, 100 ng/ml VEGF, 10 μM RA and vehicle. VEGFR-2 co-localization with early endosomes (EEA1 positive) and recycling endosomes (Rab11 positive) was assessed by immunostaining.

Results: Both calcitriol and RA stimulated internalization of VEGFR-2 into early endosomes similarly to VEGF, while they had no effect on recycling (**Figures 6 and 7**).

Figure 3. Effects of calcitriol (D3) on the VEGF–induced increases in PV-1 protein and mRNA expression
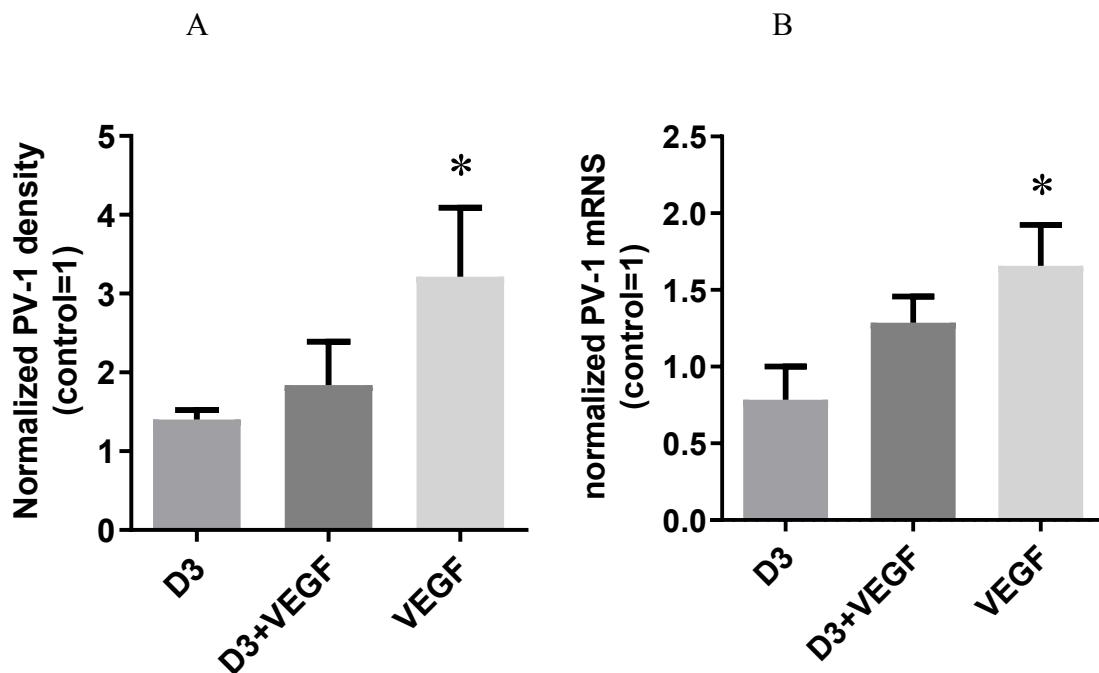
(A) Protein expression (B) mRNA expression. Confluent HUVEC monolayer was treated with 0.1 nM calcitriol, 100 ng/ml VEGF, or 0.1 nM calcitriol prior to 100 ng/ml VEGF for 48 hours (n=3). *: $p < 0.05$, VEGF vs. D3+VEGF. One-Way ANOVA, Tukey's post hoc test.

Figure 4. Calcitriol decreased the VEGF-induced upregulation of PV-1 protein expression in HUVEC cells
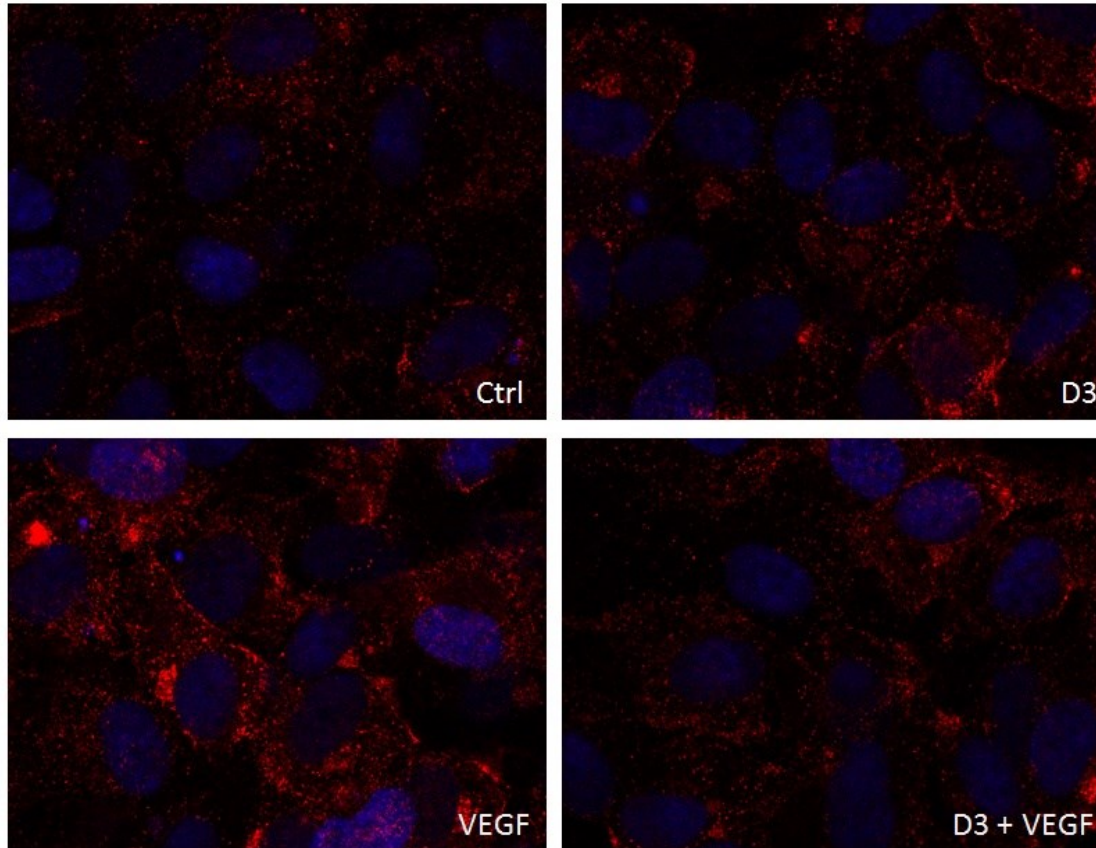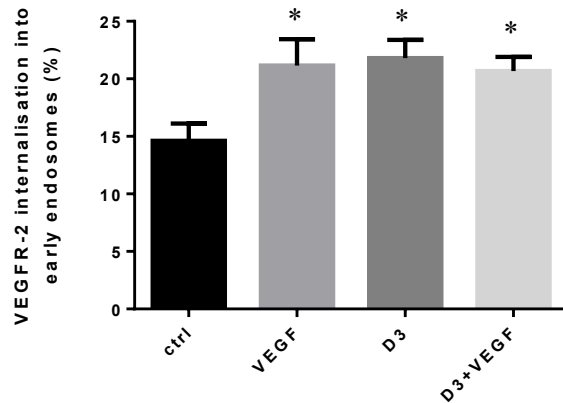

Confluent HUVEC monolayer was treated with vehicle, 0.1 nM calcitriol, 100ng/ml VEGF or co-treated with calcitriol and VEGF for 48 hours. PV-1 protein (red) and nuclei (blue) were co-stained.

**Figure 5. Calcitriol inhibited the phosphorylation of VEGF receptor-2 at Tyrosine 1175**
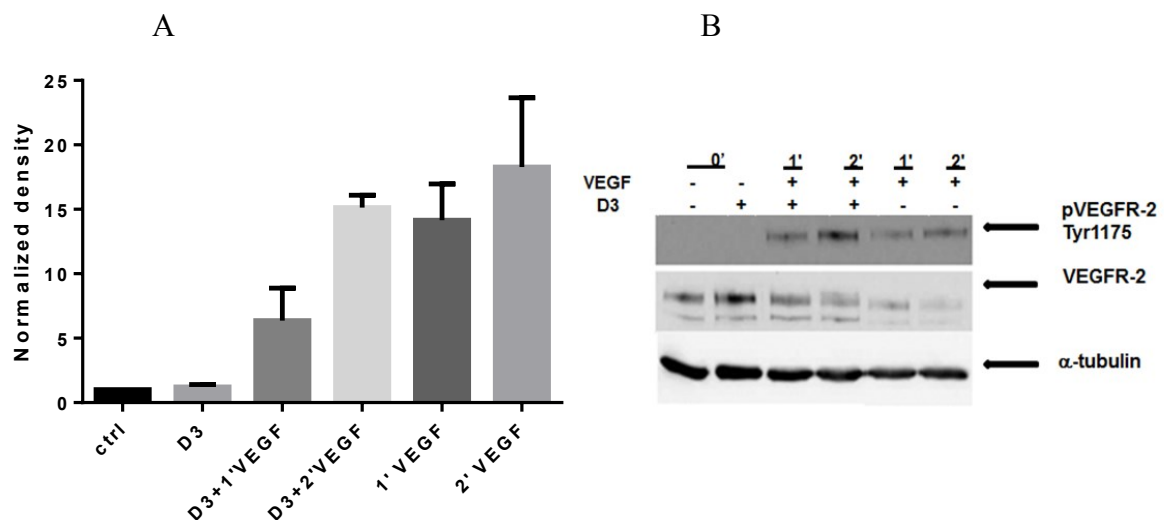
(A) Confluent HUVEC monolayer was treated with vehicle or 0.1 nM calcitriol for 30 min, and 100 ng/ml VEGF was added to the medium for 1 and 2 minutes; 0.1 nM calcitriol for 30 minutes and co-treated with 100 ng/ml VEGF for 1 or 2 minutes. (n=3/group, mean±SEM); **(B)** Representative image of phospho-VEGFR-2 western blot.

Figure 6. Calcitriol and VEGF provoke VEGF receptor-2 internalization into Early Endosome Antigen 1 (EEA1) positive endosomes as detected by immunofluorescence
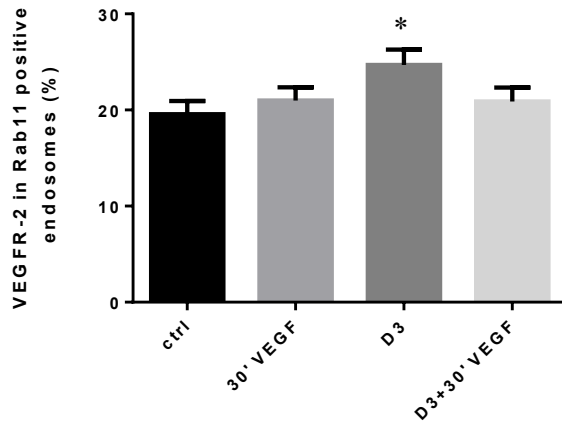

Confluent HUVEC monolayer was treated with vehicle, 0.1 nM calcitriol for 30 minutes, 100 ng/ml VEGF for 5 minutes, co-treated with 0.1 nM calcitriol for 30 minutes and 100 ng/ml VEGF for 5 minutes. HUVECs were double labeled for VEGFR-2 and EEA1. (n=12-16). One-way ANOVA and Dunnett's multiple comparisons test, $*p < 0.05$ vs control.
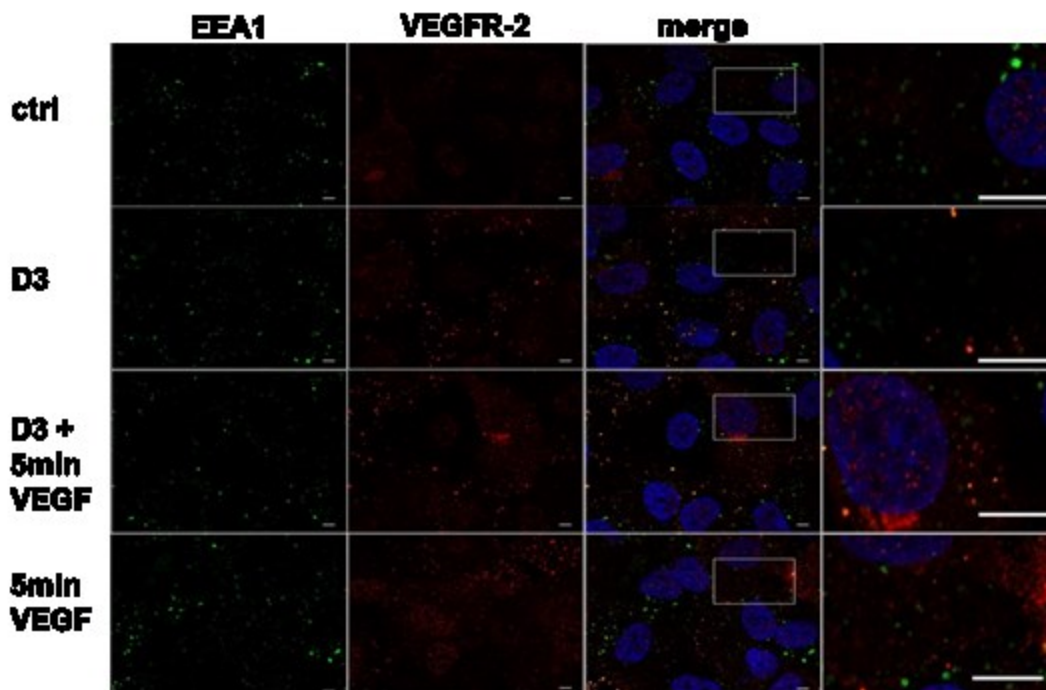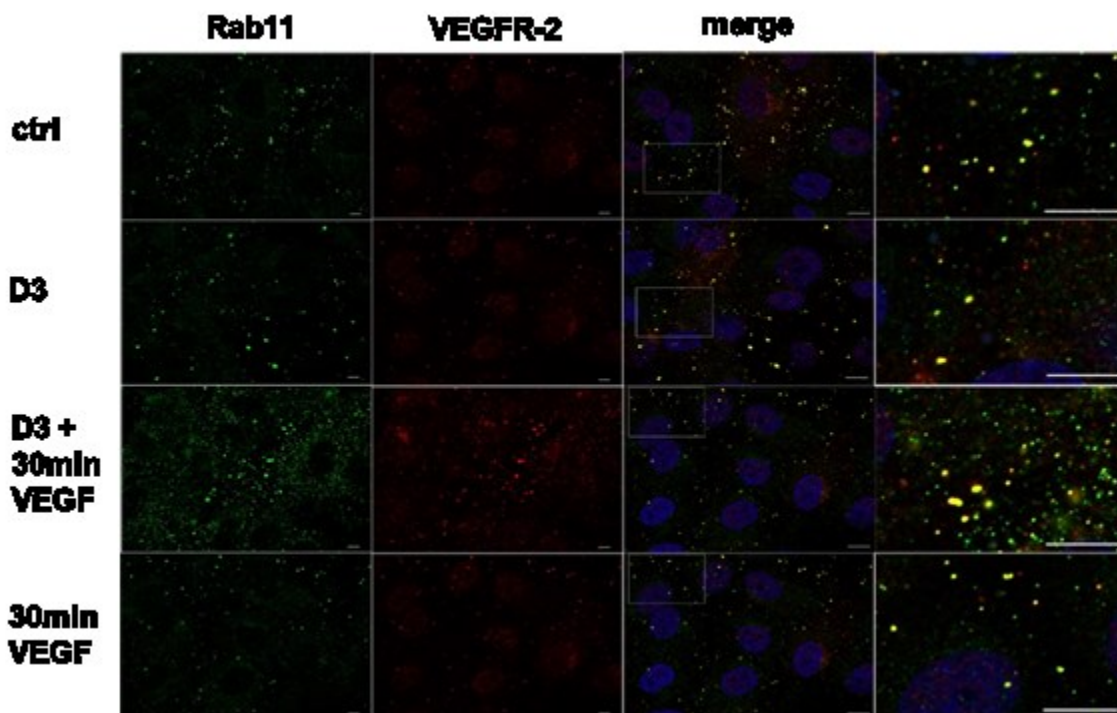

Representative examples of confocal images and their merges. VEGFR-2 labeled with A-647-conjugated secondary antibody shown is in red and EEA-1 with A488-secondary antibody is shown in green. Nuclei appear blue after DAPI staining. Scale bars, 10 μm. Images were analyzed by MetaXpress software, Multiwavelength Cell Scoring application to quantify VEGFR-2/EEA-1 co-localization. After treatment with calcitriol or VEGF the number of VEGFR-2 positive/EEA-1 positive compartments were elevated compared to vehicle treated

cells. The number of colocalizations were not altered by VEGF co-treatment (n=4). Data are mean±SEM. At least four random areas were quantified in each well.

Figure 7. Calcitriol-treatment increased the percentage of VEGFR receptor-2 in Rab11 positive endosomes (n=12)

Confluent HUVEC monolayer was treated with vehicle, 0,1 nM calcitriol for 30 minutes, 100ng/ml VEGF for 30 minutes, co-treated with 0,1 nM calcitriol for 30 minutes and 100ng/ml VEGF for 30 minutes. HUVECs were double labeled for VEGFR-2 and Rab11. One-way ANOVA and Dunnett's multiple comparisons test, *p < 0.05 vs control.

Representative examples of confocal images and their merges. VEGFR-2 labeled with A-647-conjugated secondary antibody is shown in red and Rab11 with A488-secondary antibody is shown in green. Nuclei appear blue after DAPI staining. Scale bars, 10 μm. Images were analyzed by MetaXpress software, Multiwavelength Cell Scoring application to quantify VEGFR-2/Rab11 co-localization. After treatment with calcitriol or VEGF the number of VEGFR-2 positive/Rab11 positive compartments were elevated and compared to the vehicle

treated wells. The number of co-localization was not altered by VEGF co-treatment (n=3). Data are mean±SEM. At least four random areas were quantified in each well.

2.1.6 Effects of calcitriol on FITC-Dextran permeability in CiGENC cells

In order to establish the effects of calcitriol on the cellular permeability of CiGENC cells, we determined the dose response curve of calcitriol.

Results: To our surprise, calcitriol produced a U-shaped dose response curve, i.e. calcitriol slightly increased the permeability at 0.01 nM, had no effects at 0.1 and 1.0 nM, while calcitriol increased the permeability of CiGEnC cells to FITC-Dextran by about 20 % at 10 nM.

2.1.7 Impedance changes in CiGENC cells after treatment with VEGF

Electric Cell-substrate Impedance Sensing (ECIS) is a real-time, impedance-based cell monitoring technology to study the changes in cell permeability after administration of various test substances to cells grown in culture. The cells were proliferated at 33C for 4 days and differentiated at 37 C for 5 days.

Results: The current study evaluated the effects of VEGF at 100 nM on the permeability of CiGENC cells under two conditions: first when the medium was fully changed for a fresh medium containing VEGF at 100 nM; second, concentrated VEGF was added to the medium to yield a final VEGF concentration of 100 nM. The reason to compare the two conditions is that changing the medium or even the addition of some extra amount of fluid to the medium caused great disturbance to the cells. Therefore, this comparison allows us to determine the more reliable method for treating CiGENC cells in the ECIS system. Impedance of CiGENC cells, reflecting permeability, decreased in both cases 48 hours after treatment the cells with VEGF. Cell permeability increased more without full medium replacement 7.6±1.0 vs. 5.5±0.5, p<0.05. In conclusion, VEGF increased the cell permeability in both conditions but full medium replacement is not advisable.

4   The correlation between the length of fenestrated segment of AA and the animal model of renal fibrosis

4.1 The correlation between the length of fenestrated segment of AA and the renal tissue lesion in TGF-beta transgenic mice.

Previously we have shown that PV-1 was intensively immune-labelled in confluent human umbilical vein endothelial cell (HUVEC) monolayers. Now we have started to introduce the technique in mouse and rat kidney sections in order to evaluate the length of PV-1 positive AA segments in various disease models and in our special TGFβ overexpressing, CKD prone mouse strain. The method can also be used to make a semi-quantitative estimate of the relative density of PV-1, which may correlate with the number of fenestrations in endothelial cells.

Results: So far, the sensitivity of immunohistochemistry was insufficient to demonstrate PV-1 protein in the AA of mice. We plan to by new PV-1 antibody and change for fluorescent detection in order to increase sensitivity. Certainly, the length of the fenestrated endothelium and the length of JGA cells strongly correlate. So if our new attempt to visualize the fenestrated endothelium in the afferent arterioles of mouse kidneys fails, we can measure the length of renin secreting cells along the afferent arterioles, which can provide practically the same information.

4.2 The role of (pro)renin receptor blockade on the filtration barrier in diabetic rats

Diabetic nephropathy is characterized by permeability changes of the glomerular capillary network and the filtration barrier, which leads to proteinuria. The mainstream therapy of diabetic nephropathy includes the blockade of the renin-angiotensin system (RAS) but the role of the (pro)renin receptor as a potential therapeutic target is not known. We compared the renal effects of (pro)renin receptor ((P)RR) blockade and angiotensin converting enzyme (ACE) inhibition on the progression of diabetic nephropathy in rats. Diabetes (DM) was induced by i.p. streptozotocin in adult male Sprague-Dawley rats, followed by an eight-week treatment with the (P)RR blocker „handle region" decoy peptide (HRP, 0.1 mg/kg/day, osmotic minipumps) or with the ACE inhibitor Quinapril (Q, 50 mg/kg/day in the drinking water) in the following groups: 1. Control, 2. DM, 3. DM+HRP, 4. DM+Q, 5. DM+Q+HRP.

Results: HRP reduced glomerulosclerosis index but did not affect proteinuria. Both Q and Q+HRP treatment reduced proteinuria, glomerular and tubular damage. The effect of HRP was partially beneficial on diabetic kidney injury as HRP reduced glomerular but did not improve tubular damage. These results seem to suggest that (pro)renin receptor blockade can partly reverse glomerular injury without altering the permeability of the glomerular capillary network and filtration barrier in diabetic nephropathy.

4.3 The role of renal nerves in renin secretion and plasma aldosterone levels in rats fed a low potassium diet

The renal nerves effectively regulate renin secretion in the juxtaglomerular cells. It has been shown recently that renal sympathectomy slowed the progression of heart failure in patients by inhibiting RAS. Potassium intake is frequently inadequate in patients of developed countries. Therefore, we studied the effects of chronic bilateral renal denervation (BRD) on the activity of the ARS and blood pressure in rats fed a potassium deficient diet. We also plan to study the effects of BRD on the afferent arteriolar endothelium using immunohistochemical methods. BRD was performed in male Wistar rats and after a one-week recovery they were put on a control (NP) or potassium deficient (LP) diet (K+: NP=179 mM/kg, LP=13 mM/kg) for 7 days. Blood pressure (BP) was recorded in the conscious state in acutely cannulated rats. Blood was taken for measuring plasma electrolytes, plasma renin activity (PRA) and aldosterone concentration.

Results: LP decreased plasma potassium concentration (NP=4.4±0.3, LP=3.0±0.1 mmol/L; p<0.05) and resulted in a compensated metabolic alkalosis. BP was lower in rats with chronic BRD (SO=102.8±2.9, BRD=93.5±2.3 mmHg; p<0.05), PRA (SO=13.5±1.9, BRD=6.8±1.3 ng/ml/h; p<0.05), and plasma aldosterone concentration (SO=12.7±1.2, BRD=9.4±0.5 ng/dl; p<0.05) decreased in rats with BRD compared to SO. Chronic bilateral renal denervation decreased blood pressure and plasma aldosterone concentrations in normotensive rats at least in part due to decreased plasma renin activity. We might assume that filtration from the permeable portion of afferent arteriole into the JGA interstitium decreased during these experimental conditions due to the changes in renal renin activity.

Conclusions

Ang II is an important regulator of endothelial permeability and fenestrae formation. Now we have established that other components of RAS are also involved in the regulation of endothelial function. Renin, Ang III and Ang IV can also increase PV-1 protein expression in HUVEC, which is likely the consequence of increased fenestra formation. Since the endothelium can synthesize angiotensinogen the effects of renin and prorenin should be studied in more detail as they can increase the levels of other components of RAS. Ang II had a greater effect on PV-1 expression in CiGENC than VEGF, while their effect was similar in

HUVEC. Thus, CiGENC can be a better cell type to study the effects of RAS on the regulation of endothelial permeability and fenestrae formation. Acute effects of Ang II were significant on PV-1 expression and permeability as well. RAS can have multiple roles in the regulation of endothelial permeability and fenestrae formation in the kidney, which finding can extend our understanding of renal physiology and pathophysiology.

As a first step in the elucidation of detailed mechanisms of the effects of calcitriol in the regulation of endothelial permeability and fenestrae formation we have demonstrated that VEGFR-2 Tyr1175 was trans-phosphorylated 1 and 2 min after treatment with VEGF and this effect was attenuated by calcitriol. Accordingly, chronic effects of calcitriol on endothelial permeability might involve VEGFR-2 transactivation and downstream signaling. VEGFR-2 is localized to the plasma membrane and after ligand binding VEGFR-2 receptors are internalized to become activated. Then the fate of VEGFR-2 is recycling or degradation. We have also shown that retinoic acid and calcitriol increased VEGFR-2 internalization on their own, which shows that these two agents might modulate VEGFR-2 trafficking.

There is surprising growth in the number of the components of RAS. More and more active metabolites are recognized with their own receptors proving the importance of this system in the regulation of fluid balance, blood pressure, microcirculation, immune system, etc. This notion provides special emphasis of these results and opens new pathways and horizon for our further research. In addition, several other agent such as retinoic acid, calcitriol and VEGF, may modulate these regulatory effects.

An important conclusion from the current set of experiments is that blockade of the angiotensin II type 1a receptors using losartan decreased capillary permeability in the skin and lung of mice on a normal sodium intake, when the activity of the RAS is normal, but such effects were abolished by high sodium intake, which suppresses renin activity. It was unexpected that sodium chloride restriction, when the RAS is activated, inhibition of the angiotensin II type 1a receptors increase plasma extravasation only in the skin. Concerning the mRNA and protein expression of the main components and regulatory factors of capillary permeability we have shown so far that mRNA expression of PV-1 was similar in the kidney irrespective of sodium intake. We have also shown that blockade of the (pro)renin receptors can attenuate glomerular injury in diabetic rats, but does not alter proteinuria, suggesting the (pro)renin receptor has no effect on glomerular capillary permeability and the filtration barrier. The renal nerves have a major influence on the RAS even in rats fed a potassium deficient diet, which observation prompts us to further evaluate the effects of renal nerves on the endothelial morphology and function in the afferent arteriole and juxtaglomerular cells. All these experimental conditions might have subtle effects also on the afferent arteriolar morphology and permeability even without detection of the changes with the crude methods used.